

A NOVEL METHOD FOR WATERLINE EXTRACTION FROM REMOTE SENSING IMAGE BASED ON QUAD-TREE AND MULTIPLE ACTIVE CONTOUR MODEL

Zhang Baoming, Guo Haitao, Lu Jun and Yu Jintao

Zhengzhou Institute of Surveying and Mapping, Zhengzhou 450052, China

ABSTRACT

After the characteristics of geodesic active contour model (GAC), Chan-Vese model (CV) and local binary fitting model (LBF) are analyzed, and the active contour model based on regions and edges is combined with image segmentation method based on quad-tree, a waterline extraction method based on quad-tree and multiple active contour model is proposed in this paper. Firstly, the method provides an initial contour according to quad-tree segmentation; secondly, a new signed pressure force (SPF) function based on global image statistics information of CV model and local image statistics information of LBF model has been defined, and then, the edge stopping function(ESF) is replaced by the proposed SPF function, which solves the problem such as evolution stopped in advance and excessive evolution; finally, the Selective Binary and Gaussian Filtering Level Set method is used to avoid reinitializing and regularization to improve the evolution efficiency. The experimental results show that this method can effectively extract the weak edges and serious concave edges, and owns some properties such as sub-pixel accuracy, high efficiency and reliability for waterline extraction.

KEYWORDS

Quad-tree; GAC model; CV model; LBF model; Waterline extraction

1. INTRODUCTION

The waterline extraction for coastal zone and island (reef) image is the basis to obtain the marine-oriented geographical information by remote-sensing image, and the waterline thematic map got through this way is the key data [1-2] for analyzing the coastal evolution and the integrated coastal management. The waterline extraction is the key technology for coastline extraction [3-4], and it is with significant importance to detect and extract the navigation landmarks and navigation targets on remote-sensing image. Currently, there are various methods to extract the waterline from remote-sensing images. The most commonly used extraction methods include thresholding segmentation [5], edge detection method [2], active contour model method [6-8], level-set method [1], region growing method [9], etc. The thresholding segmentation method is simple to accomplish, with faster processing rate, but it is only suitable for segmenting the image with sharp contrast between the waters and the background. The position of the waterline extracted by

the edge detection method is accurate, but the edge detected often contain disconnections, where subsequent edge processing is required; the level-set method is featured with strong anti-noise capacity, and the adaptivity of the curve topological changes is better, but with complicated algorithm, and its detection speed is relatively slow; the region growing method is capable to obtain intact waterline, but with unsatisfactory anti-noise performance, and the sudden change in the gray level of individual pixel near the seed pixel is prone to result in the skewing of the waterline easily[10]. The existing waterline extraction methods have three shortcomings [7] [11-12]: firstly, the extraction of weak edge waterline without obvious changes in gray level is not accurate; secondly, it is not easy to extract the waterline with complicated boundary accurately, especially the waterline with serious concave; thirdly, the seed region is required to be selected manually, with low automation and low efficiency. Therefore, it is hard to meet the requirements of follow-up study and automatic mapping.

The essence of waterline extraction is the segmentation of ocean-continent image. In recent years, the active contour model has been widely used in image segmentation [8-12]. This approach can be divided into boundary-based model and region-based model according to different driving force. Usually, the boundary-based active contour model utilizes the image gradient to construct the edge stopping function, thus ensuring to stop evolution at the contour of the target boundary; however, as this method utilizes the gradient information, it is hard for the evolution to stop at the target contour for the weak edge without obvious gradient changes [13], and the geodesic active contour(GAC) model is a typical boundary-based active contour model[10]. In terms of the region-based active contour model, the driving force of the contour model is based on the region statistical information of the image for construction; therefore, it is featured with better efficiency in segmentation of weak edge targets without obvious gradient or discrete boundary targets[13], and Chan-Vese (CV) model [12] is a typical region-based active contour model, and it is not sensitive to the initialization of the contour, but it cannot process the images with uneven gray level. Therefore, Li et al. proposed the regional variable active contour (LBF) model [14-15], which overcomes the shortcomings of CV model that it cannot segment the images with uneven gray level, but it is required to make convolution calculations, with large calculated amount, and it is more sensitive to the initialization of the contour. On such basis, the domestic and foreign scholars began to integrate the gradient information and the region information [16], integrate the local statistics and the global statistics [17], complement each other's advantages, and obtained better segmentation efficiency. The level-set method is the waterline extraction method for remote-sensing images of the coastal zone that has been studied more in recent years [1][6-8], especially the geometric active contour model method that integrates the level-set method and the active contour model, which is ideal for the waterline extraction by remote-sensing image. Literature [6] proposed an automatic ocean-land image segmentation method integrating the quad-tree and geometric active contour model, realizing the automatic rapid segmentation of the ocean-land image, but the segmentation effectiveness of the weak edge is not satisfactory; Literature [7] proposed a waterline extraction method based on Canny edge detection and GAC model, which has a better extraction efficiency for weak edge, and it is capable to extract the waterline with serious concave; however, the seed region is required to be selected manually, with low automation and long segmentation time. Literature [8] proposed an ocean-land image segmentation method integrating the quad-tree and the geodesic active contour model, which not only realizes the automatic rapid extraction, but also can extract the weak edge and the waterline with serious concave edges accurately, and by now, it is a method with better waterline extraction effectiveness that has been published newly.

Based on the analysis on the above methods, on the basis of analysis and study on GAC, CV and LBF model, this paper proposes a waterline extraction algorithm based on quad-tree and multiple active contour models, which can extract the weak edges and the waterlines with serious concave edges, with faster extraction speed and better stability.

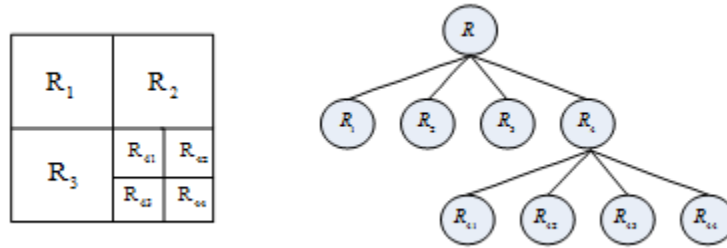
2. WATERLINE EXTRACTION PRINCIPLE BASED ON QUAD-TREE AND MULTIPLE ACTIVE CONTOUR MODELS

2.1. Ocean-land image segmentation based on Quad-tree

In terms of the ocean-land remote-sensing image, the pixel gray value of its ocean part has a certain homogeneity and better connectivity, but on the whole, the grayscale is distributed unevenly, and the image edge has rich features as a whole relative to the sea area, especially the ocean-land boundary. According to this feature, the gradient is relatively small at the sea, while the gradient at the ocean-land boundary is relatively large; therefore, in order to facilitate the subsequent segmentation, the image gradient drawing shall be constructed first in accordance with Formula(1) [6]

$$G_{i,j} = \left[(g_{i,j} - g_{i+1,j})^2 + (g_{i,j} - g_{i,j+1})^2 \right]^{\frac{1}{2}} \quad (1)$$

The essence of the quad-tree segmentation is the integration of the regional divisions and the consolidation technology with the structure of the quad-tree, thus segmenting the image. The segmentation principle is as shown in Figure 1[6], and its advantage lies in the faster segmentation speed, and it is an automatic segmentation; however, it is unable to extract the weak edges and the serious concave edges accurately.



(a) Distinguished Images (b) Corresponding Quad-tree Structure

Fig.1 Structure Diagram for Quad-tree Segmentation

2.2. CV Model, LBF Model and GAC Model

(1) CV Model

The energy function of the CV model is [12]

$$E^{CV} = \lambda_1 \int_{inside(C)} |I(x,y) - c_1|^2 dx dy + \lambda_2 \int_{outside(C)} |I(x,y) - c_2|^2 dx dy \quad (2)$$

Whereas, $I(x, y)$ indicates the original image, and λ_1 and λ_2 are constants with positive value, in general, their value can be taken as $\lambda_1 = \lambda_2 = 1$. c_1 and c_2 indicate the mean value of the image grayscale inside and outside the contour curve respectively, with the calculation formula as follows:

$$\left\{ \begin{array}{l} c_1(\phi) = \frac{\int_{\Omega} I(x, y) H_{\varepsilon}(\phi(x, y)) dx dy}{\int_{\Omega} H_{\varepsilon}(\phi(x, y)) dx dy} \\ c_2(\phi) = \frac{\int_{\Omega} I(x, y) (1 - H_{\varepsilon}(\phi(x, y))) dx dy}{\int_{\Omega} (1 - H_{\varepsilon}(\phi(x, y))) dx dy} \end{array} \right. \quad (3)$$

Whereas, the $H_{\varepsilon}(\phi(x, y))$ is the regularization of the Heaviside function, with its calculation formula as Formula (5), and $\phi(x, y)$ is the level set function.

In order to avoid the small and isolated areas as well as zero level set in the segmentation results in the end, this paper introduces the length penalty term and area penalty term, and obtains the evolution equation of the level set as follows:

$$\frac{\partial \phi}{\partial t} = \delta(\phi) \left[\mu \nabla \left(\frac{\nabla \phi}{|\nabla \phi|} \right) - \nu - \lambda_1 |I(x, y) - c_1|^2 + \lambda_2 |I(x, y) - c_2|^2 \right] \quad (4)$$

Whereas, μ is a constant greater than 0, ν is usually taken as 0, ∇ is the gradient operator, $\delta(\phi(x, y))$ is the regularization of Dirac function, with the calculation formula as shown in Formula (5)

$$\left\{ \begin{array}{l} H_{\varepsilon}(z) = \frac{1}{2} \left(1 + \frac{2}{\pi} \arctan\left(\frac{z}{\varepsilon}\right) \right) \\ \delta(z) = \frac{1}{\pi} \cdot \frac{\varepsilon}{\varepsilon^2 + z^2}, z \in R \end{array} \right. \quad (5)$$

The CV model is a region-based active contour model, can detect weak edge target without obvious gradient changes [10]. Meanwhile, the CV model takes advantage of the global information of image; therefore, it is not sensitive to the initialization of contour, and is capable of processing the images with noise effectively. However, as this model considers the image as two constant regions, it is unable to process the image with uneven grayscale.

(2) LBF Model

The energy function of the CV model is

$$\begin{aligned}
E^{LBF} = & \lambda_1 \int_{\Omega} \int_{inside(C)} K_{\sigma}(x-y) |I(y) - f_1(x)|^2 dy dx \\
& + \lambda_2 \int_{\Omega} \int_{outside(C)} K_{\sigma}(x-y) |I(y) - f_2(x)|^2 dy dx \quad (6)
\end{aligned}$$

$x, y \in \Omega$

Whereas, the $I : \Omega \rightarrow R$ refers to the input image; λ_1 and λ_2 are constants with positive values, and the K_{σ} is the Gaussian kernel function with standard deviation of σ , f_1 and f_2 refer to the grayscale function of the local region inside and outside the image of the fitting contour respectively, with its formula as follows:

$$\begin{cases}
f_1(x) = \frac{K_{\sigma}(x) * [H(\phi)I(x)]}{K_{\sigma}(x) * H(\phi)} \\
f_2(x) = \frac{K_{\sigma}(x) * [(1-H(\phi))I(x)]}{K_{\sigma}(x) * (1-H(\phi))}
\end{cases} \quad (7)$$

In order to maintain the stability and smoothness of the evolution, usually the length and signed distance constraints are introduced for level set evolution. The LBF model utilizes the local information, thus it does not have better segmentation efficiency for the images with uneven grayscale; but with only local information, without global information involved, it is sensitive to the initial contour, and is featured with unsatisfactory anti-noise performance; what's more, it involves a great deal of calculation, thus limiting its application in practice.

(3) GAC Model

The principle of the GAC model is to minimize the following energy function

$$E^{GAC}(C) = \int_0^1 g(|\nabla IC(q)|) |C'(q)| dq \quad (8)$$

Whereas, $C(q)$ is the parameterized curve, and g is the edge stopping function.

Usually, in order to increase the evolution speed of the contour method on direction, a constant term α is added, adopting the minimum level set idea of Formula (8), and then the evolution equation of the level set is obtained as follows:

$$\frac{\partial \phi}{\partial t} = g |\nabla \phi| \left(\text{div} \left(\frac{\nabla \phi}{|\nabla \phi|} \right) + \alpha \right) + \nabla g \cdot \nabla \phi \quad (9)$$

Whereas, div refers to the divergent operator.

The GAC model relies on the edge gradient information to evaluate the curve, and is capable of processing the topology changes adaptively, provides high-precision closed segmentation curve, but it is sensitive to noise, so it is required to give initial contour manually, and is prone to get local minimum value and stops evolution for serious concave edge, thus affecting the extraction accuracy and reliability [16], as shown in Figure 2

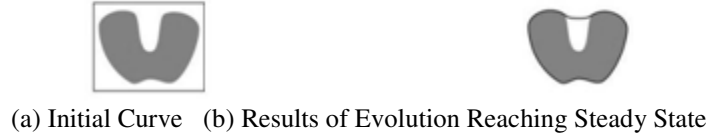


Fig.2 Local Minimum Value Problem of GAC Model

When α is small, the segmentation curve stops evolution in advance before reaching the concave edge; but when α is too large, the possibility that the contour gets across the sharp edge increases; therefore, it is unable to extract the weak edges and the serious concave edges at the same time.

2.3. Waterline Extraction Based on Quad-tree and Multiple Active Contour Models

The above-mentioned models have their own advantages and disadvantages, and how to combine them mutually, to make up each other's deficiencies and to complete the segmentation of the images jointly are the hot points and difficult points of study in recent years. Literature [16] utilizes the CV model to improve the signed pressure force function and replaces the edge stopping function of GAC model, and such improvement highlights the segmentation target, and could improve the segmentation problems of weak edges and targets with uneven grayscale, and has the capacity of evolving the curve in dual direction: when the evolution curve is within the target, the curve evolves externally; when the evolution curve is outside the target, the curve evolves internally, thus reaching the target boundary finally. The influence of the signed pressure force function on curve evolution is as shown in Figure 3. The evolution equation of the level set is as shown in Formula (10)

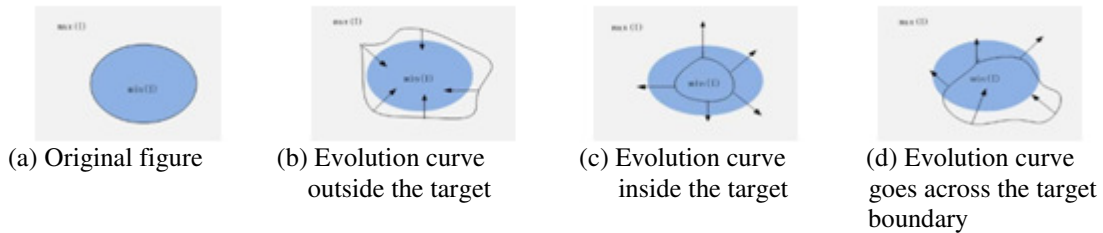


Fig.3 The Influence of Signed Pressure Force Function on Curve Evolution

$$\frac{\partial \phi}{\partial t} = spf(I) \cdot \left(\text{div} \left(\frac{\nabla \phi}{|\nabla \phi|} \right) + \alpha \right) |\nabla \phi| + \nabla spf(I) \cdot \nabla \phi \quad (10)$$

Whereas, $spf(I)$ refers to the signed pressure force function.

Su Rina et al.[18] made use of the local region statistics of LBF model to improve the signed pressure force function, and proposed a new region-based active contour model. In view that CV model is unable to segment the images with uneven gray scale, while LBF model has a better effectiveness for such images. Therefore, this paper integrates the advantages of CV and LBF model to construct a new signed pressure force function

$$spf(I) = \frac{w \cdot (I - \frac{f_1 + f_2}{2}) + (1-w) \cdot (I - \frac{c_1 + c_2}{2})}{\max(w \cdot (I - \frac{c_1 + c_2}{2}) + (1-w) \cdot (I - \frac{f_1 + f_2}{2}))} \quad (11)$$

Whereas in Formula (11), $w(0 \leq w \leq 1)$ is a weight factor, and it can make adjustment according to the details of the image and the nonuniformity of the gray scale as determined by experience. In case of many image details or uneven gray scale, the value of w shall be small enough, which can be set as 0.1; otherwise, it shall be set as larger value, usually it can be set as $w=0.7$, and then it could extract the edge better. The improved signed pressure force function can highlight the segmentation targets, and it has the capacity of dual-way evolution, thus improving the problem of GAC model effectively that it cannot extract the weak edges and serious concave edges at the same time. Therefore, the signed pressure force function constructed by this method can not only maintain the advantages of global information, and avoid the minimum evolution contour locally at the mean time during the level set evolution, but also maintain the advantages of local information, so it has a better effectiveness in the segmentation of image with uneven gray scale [16].

In Formula (11), $div(\nabla\phi/|\nabla\phi|)|\nabla\phi|$ is a regularization item, whose role is to regularize the level set function ϕ . As the level set function is a signed distance function and meets the requirement of $|\nabla\phi|=1$, then such regularization item meets the condition of $div(\nabla\phi/|\nabla\phi|)|\nabla\phi| = \Delta\phi$ [19], indicating that the regularization item can be expressed by the Laplace of the level set function ϕ . According to Literature [20] and the scale-space theory, if an evolution function evolves according to Laplace's equation, its effectiveness equates to the smoothing of gaussian kernel function for its initial contour. Therefore, the Gaussian filter can be used to replace this regularization item during the realization, and the $div(\nabla\phi/|\nabla\phi|)|\nabla\phi|$ in Formula (10) can be omitted. The re-initialization of the level set evolution has always been a difficulty for level set method, and in order to ensure the accuracy of the contour evolution, the re-initialization is applied in level set method [10], but there are errors between the theoretical and practical numerical implementation, so the re-initialization may make the zero level set deviate from its original position, and it involves a great deal of calculations, with low efficiency. In addition, it is hard to decide when and how to make initialization. Literature [17] proposed the Selective Binary and Gaussian Filtering Level Set (SBGFRLS) method is used to avoid reinitialization [21], and saves the reinitialization time, thus improving the evolution efficiency significantly. As the method adopted by this paper utilizes the region statistical information with broader boundary capture range, so the $spf(I)|\nabla\phi|$ in Formula (10) can also be omitted, and finally, the evolution equation is shown as follows:

$$\frac{\partial\phi}{\partial t} = spf(I) \cdot \alpha |\nabla\phi| \quad (12)$$

It can be seen from the above analysis that, the image segmentation algorithm based on quad-tree is featured with rapid segmentation speed and high level of automation, but it cannot segment the weak edges and serious concave edges accurately; therefore, this paper adopts the thoughts segmenting the given initial contour with quad-tree roughly at first, and then utilizing the multiple

active contour models for fine segmentation so as to get accurate results. This method can not only extract general waterline accurately, but also can extract the weak edges and the waterlines with serious concave edges.

The algorithm flow for waterline extraction based on quad-tree and multiple active contour models is as shown in Figure 4.

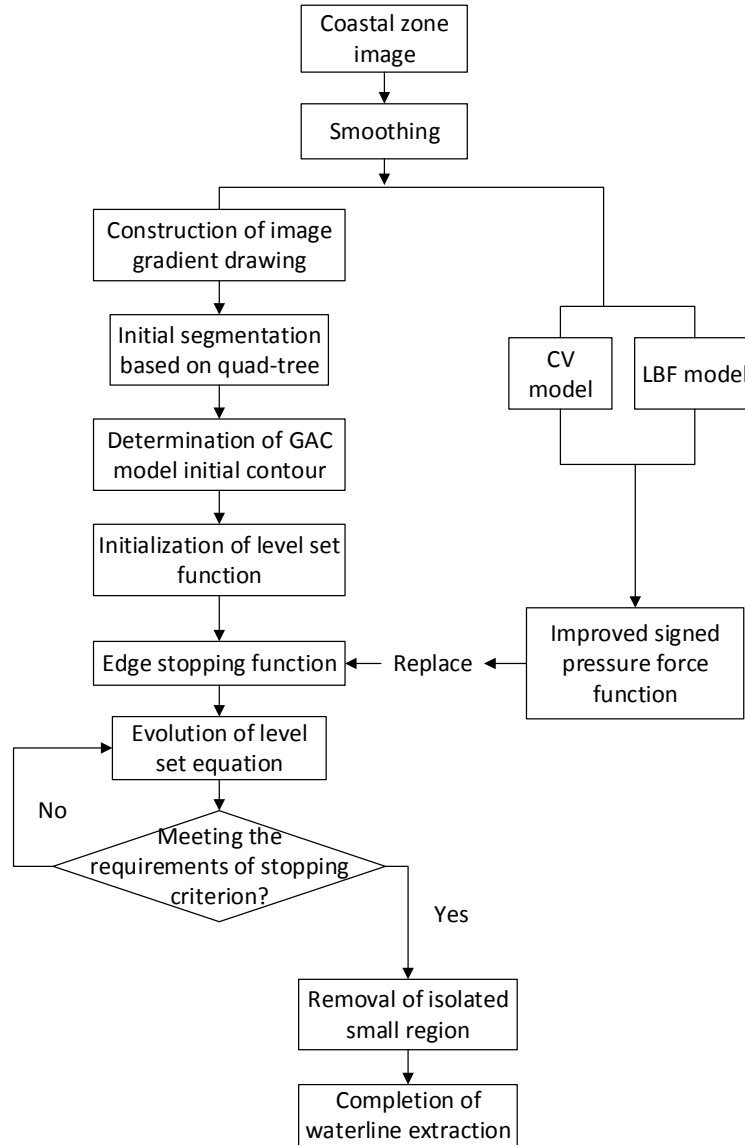


Fig.4 Flowchart for waterline extraction

3. EXPERIMENTAL FINDINGS AND ANALYSIS

In order to verify the effectiveness of the algorithm proposed by this paper, multiple groups of experiments were conducted, and analysis was also made to compare with other 3 waterline extraction methods. In order to analyze the extraction efficiency of these four methods quantitatively, 6 groups of experiments were listed below, which made statistics and verification from four aspects, including extraction precision, number of iterations, operation times and extraction accuracy. In terms of the extraction accuracy, the methods made use of the evaluation methods that were widely used by line feature extraction for quantitative evaluation analysis, and compared the waterlines extracted by each algorithm and by manpower (or the actual), and then evaluated the accuracy of the extraction results from completeness (CP), accuracy (CR) and extraction quality (QL). Please refer to Literature [22] for the calculation method. Experiment 1 adopted standard edge simulation images to verify the sub-pixel extraction accuracy by the algorithm in this paper; Experiment 2 made use of QuickBird images to verify the algorithm in this paper; Experiment 3, 4, 5 and 6 made use of the panchromatic and multispectral images of Mapping Satellite to verify the algorithm in this paper, and compared and tested the waterline extraction methods proposed in [6-8].

3.1. Standard Edge Simulation Image Experiment

In order to evaluate the accuracy of the algorithm proposed by this paper simply and accurately, Experiment 1 adopted the standard edge simulation images with known extraction results for verification. Based on CCD image-forming principle, the ideal step-shaped edge[23] was formed according to the sampling theorem of square aperture, and the experiments were carried out on six standard edge images of 10° , 15° , 35° , 45° , 60° and 75° , with image size of 201×201 , and the experiment results were as shown in Figure 5, and (a)-(f) were the extraction results of the above six standard image edges generated according to the method proposed in [23] by the method proposed in this paper. The extraction accuracy adopted the method proposed in [24] for quantitative calculation, which is to evaluate the extraction accuracy by average distance value of various edge points and theoretical edge line. The extraction accuracy of standard edge image at different angles by the method proposed in this paper is as shown in Table 1.

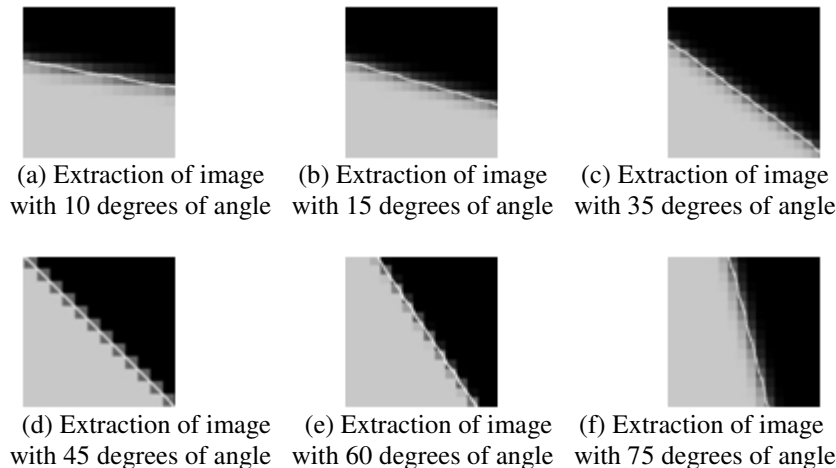


Fig.5 Accuracy Verification for Sub-pixel Extraction in Experiment 1

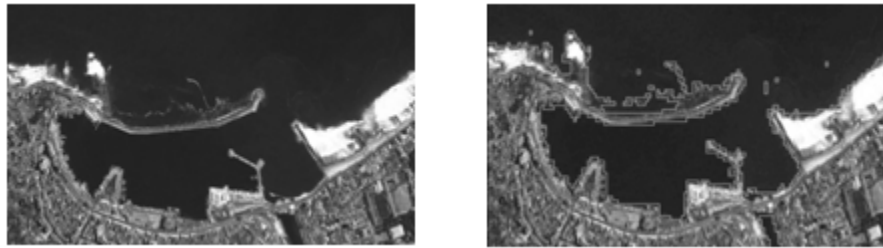
Table.1 Results of Different Angles Standard Image Extraction in Experiment 1

Angle of Inclination	10	15	35	45	60	75
Extraction Precision / Pixel	0.054	0.02	0.036	0.041	0.043	0.041

It can be seen from Table 1 and Figure 5 that, the extraction accuracy achieved by the method proposed in this paper can fall within 0.1pixel, indicating that the accuracy extracted by the algorithm of this paper reaches sub-pixel level. The experiments were also made for the ideal roof-style and line-type edge, which all had proved that the extraction accuracy achieved by the algorithm proposed in this paper could reach the sub-pixel level.

3.2. QuickBird Images Experiment

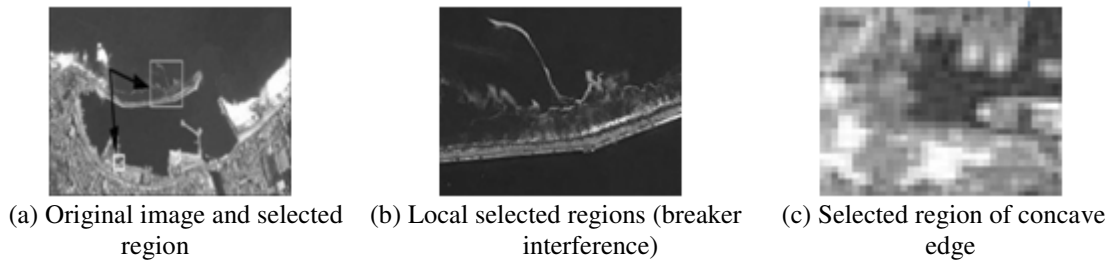
Experiment 2 adopted the QuickBird satellite images of Dalian region obtained in 2014 as the experimental data, with resolution of 0.61m, the size of 1173× 719 pixels, and the quad-tree segmentation results were as shown in Figure 6 below. This experiment made comparison and tested the extraction capacity of the algorithm proposed in this paper in operating efficiency, weak edges and serious concave edges. The experimental results are as shown in Figure 7 below, (a) - (c) in Figure 7 refer to the selected region of original image, the weak edge and the concave edge respectively; (d)-(f) refer to the extraction results of the original image, the weak edge and the concave edge obtained by the method proposed in [6] respectively; (g)-(i) refer to the extraction results of the original image, the weak edge and the concave edge obtained by the method proposed in [7] respectively; (j)-(l) refer to the extraction results of the original image, the weak edge and the concave edge obtained by the method proposed in [8] respectively. (m)-(o) refer to the extraction results of the original image, the weak edge and the concave edge obtained by the method proposed by this paper.



(a) Original image

(b) Quad-tree segmentation results

Fig.6 Results of Quad-tree Segmentation



(a) Original image and selected region

(b) Local selected regions (breaker interference)

(c) Selected region of concave edge

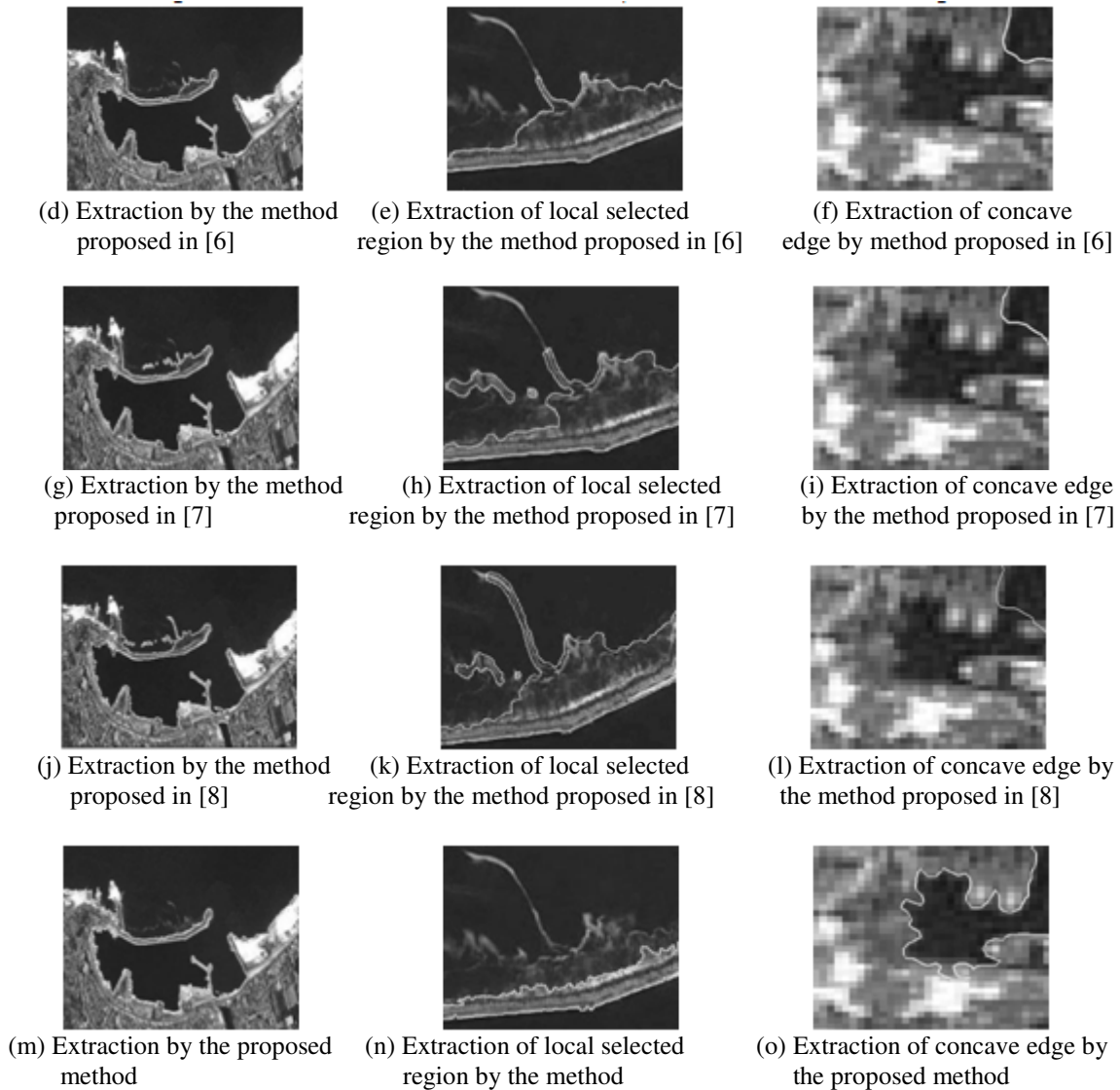


Fig.7 Results of Waterline Extraction in Experiment 2

As can be seen from Figure 6, the contour obtained by quad-tree segmentation is very close to the real waterline, and provides precise initial contour for level set evolution, reduces the number of evolution and improves the efficiency of the evolution. It can be seen from the experimental results of the second column in Figure 7, the extraction edge obtained by the method specified in Literature [6-8] differed greatly from the actual edge under the interference of breaker, the extraction results were not accurate, and its capacity to extract the waterline of serious concave edges was also poor; while the method proposed by this paper has a better efficiency even under the interference of breaker, and its extraction results are closer to the actual edge, and is capable to extract the serious concave edges accurately. Meanwhile, its extraction efficiency is significantly higher than the method specified in Literature [6-8], and the statistics about the operating efficiency and extraction accuracy are as shown in Table 2.

Table.2 Operating Efficiency and Extraction Accuracy for Each Algorithm in Experiment 2

Methods	Number of Iterations/Time	Operating Time/Sec	CP/%	CR/%	QL/%
Method proposed in [6]	480	106.7	87.0	91.1	77.3
Method proposed in [7]	1940	434.5	85.0	86.3	72.3
Method proposed in [8]	430	91.5	85.0	86.3	72.3
The proposed method	140	23.4	97.4	99.4	97.0

3.3. Mapping Satellite - I Satellite Image Experiment

Experiment 3 adopted the images of Dalian region obtained by Mapping Satellite in 2014 as the experimental data, with the size of 498×427 pixels and resolution of 2m.

This experiment made comparison and tested the extraction accuracy of the algorithm proposed in this paper in operating efficiency and general waterline. The experimental results are as shown in Figure 8 below, (a) in Figure 8 refers to the original image, (b)-(d) indicate the extraction results of the original images made according to the method specified in Literature [6-8] and in this paper respectively; (e) Enlarged image of the selected region, (f)-(h) indicate the extraction results of the selected region made according to the method specified in Literature [6-8] and in this paper respectively. The statistical results about the operating efficiency and extraction accuracy are as shown in Table 3.

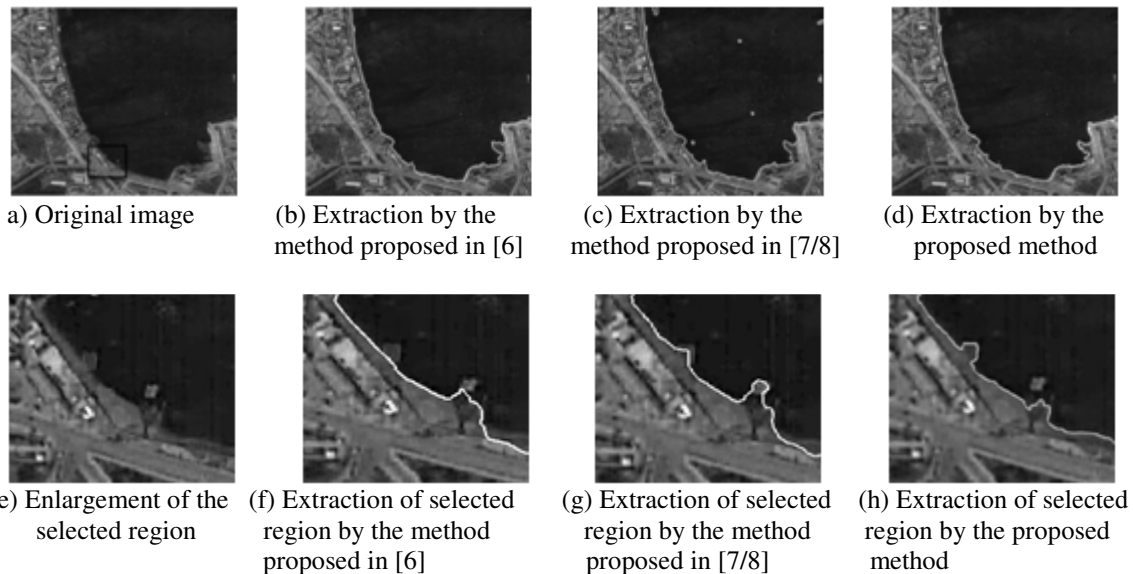


Fig.8 Results of General Waterline Extraction in Experiment 3

Experiment 4 adopted the images of Dalian region obtained by Mapping Satellite in 2014 as the experimental data, with the size of 811×639 pixels and resolution of 2m. This experiment made comparison and tested the extraction accuracy of the algorithm proposed in this paper in operating efficiency and serious concave waterline. The experimental results are as shown in Figure 9 below, (a) in Figure 9 refers to the original image, (b)-(d) indicate the extraction results

of the original images made according to the method specified in Literature [6-8] and in this paper respectively; (e) Enlarged image of the selected region, (f)-(h) indicate the extraction results of the selected region made according to the method specified in Literature [6-8] and in this paper respectively. The statistical results about the operating efficiency and extraction accuracy are as shown in Table 4.

Table.3 Operating Efficiency and Extraction Accuracy for Each Algorithm in Experiment 3

Methods	Number of Iterations/Time	Operating Time/Sec	CP/%	CR/%	QL/%
Method proposed in [6]	200	10.6	93.0	97.0	90.0
Method proposed in [7]	680	37.4	95.8	96.2	92.1
Method proposed in [8]	140	7.3	95.8	96.2	92.1
The proposed method	60	2.5	99.7	100.0	99.7

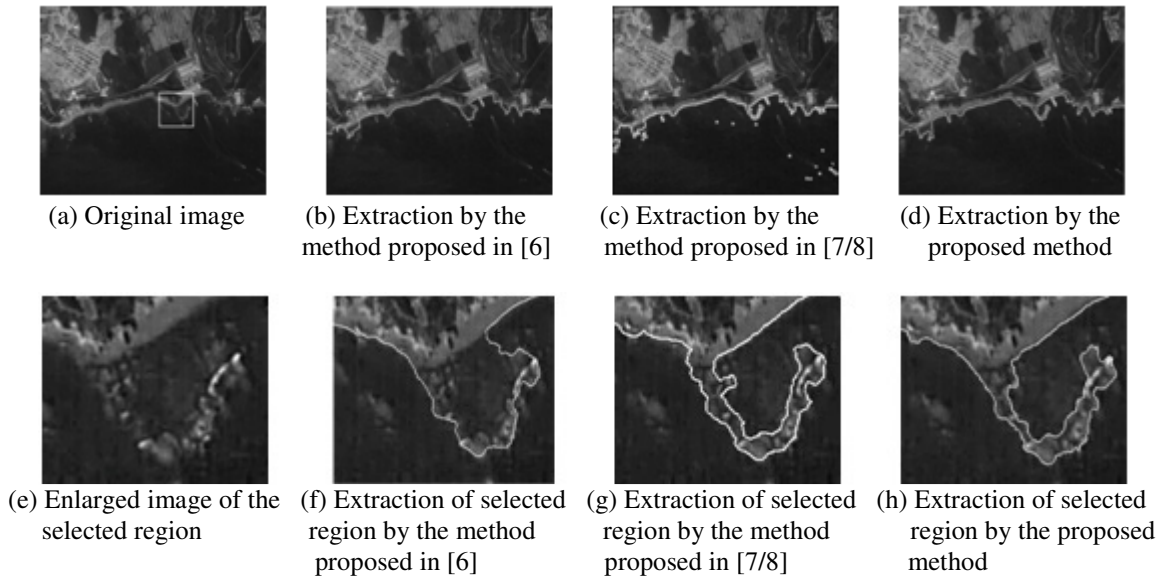


Fig.9 Experimental Results of Waterline Extraction for Concave Edges

Table.4 Operating Efficiency and Extraction Accuracy for Each Algorithm in Experiment 4

Methods	Number of Iterations/Time	Operating Time/Sec	CP/%	CR/%	QL/%
Method proposed in [6]	960	131.0	76.9	89.6	69.1
Method proposed in [7]	1020	138.6	78.7	86.6	69.3
Method proposed in [8]	900	120.6	78.7	86.6	69.3
The proposed method	220	23.2	97.4	99.0	96.2

Experiment 5 adopted the images of Dalian region obtained by Mapping Satellite in 2014 as the experimental data, with the size of 859×710 pixels and resolution of 2m. This experiment made comparison and tested the extraction accuracy of the algorithm proposed in this paper in operating efficiency and waterline of weak edges. The experimental results are as shown in Figure 10 below, (a) in Figure 10 refers to the original image, (b)-(d) indicate the extraction results of the original images made according to the method specified in Literature [6-8] and in this paper respectively; (e) Enlarged image of the selected region, (f)-(h) indicate the extraction results of the selected region made according to the method specified in Literature [6-8] and in this paper respectively. The statistical results about the operating efficiency and extraction accuracy are as shown in Table 5

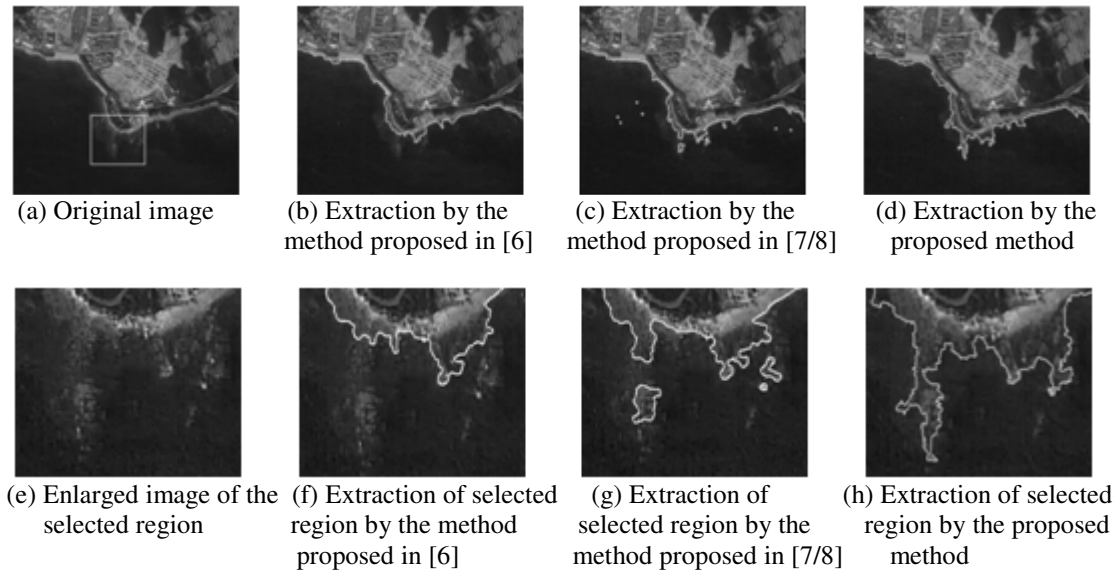


Fig.10 Experimental Results of Waterline Extraction for Weak Edges

Table.5 Operating Efficiency and Extraction Accuracy for Each Algorithm in Experiment 5

Methods	Number of Iterations/Time	Operating Time/Sec	CP/%	CR/%	QL/%
Method proposed in [6]	440	69.3	67.1	83.1	58.5
Method proposed in [7]	1740	275.8	65.8	84.5	58.9
Method proposed in [8]	420	65.2	65.8	84.5	58.9
The proposed method	100	12.2	90.8	96.1	88.2

Experiment 6 adopted the multispectral images of Mapping Satellite as the experimental data, with the size of 980×588 pixels and resolution of 10m. This experiment made comparative tests for the multispectral images. The experimental results are as shown in Figure 11 below, (a) in Figure 11 refers to the original image, (b)-(d) indicate the extraction results of the original images made according to the method specified in Literature [6-8] and in this paper respectively; (e) Enlarged image of the selected region, (f)-(h) indicate the extraction results of the selected region made according to the method specified in Literature [6-8] and in this paper respectively. The statistical results about the operating efficiency and extraction accuracy are as shown in Table 6.

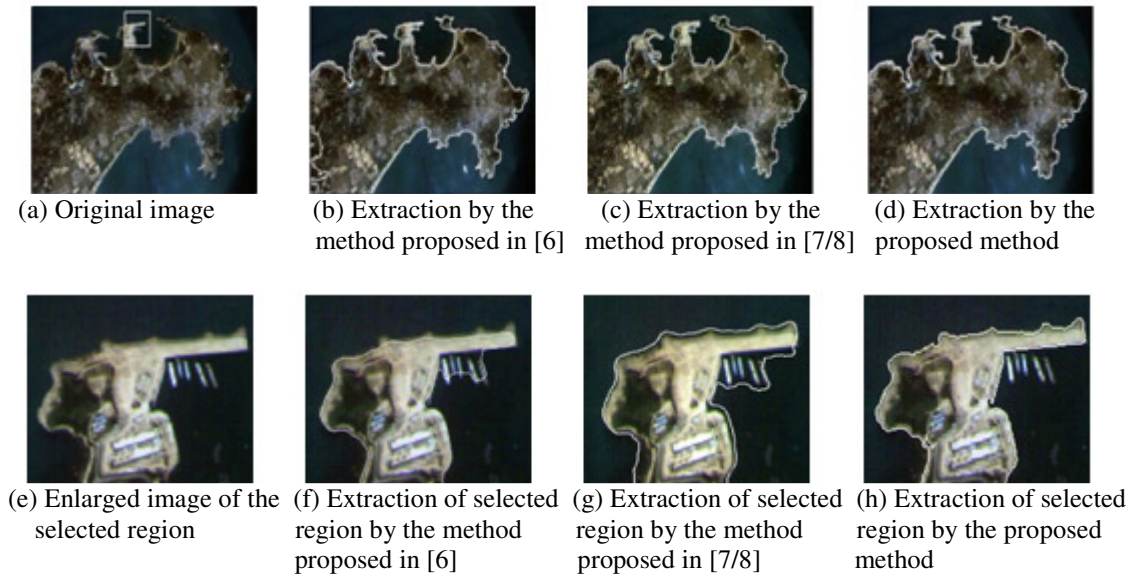


Fig.11 Experimental Results of Multispectral Image Waterline Extraction

Table.6 Operating Efficiency and Extraction Accuracy for Each Algorithm in Experiment 6

Methods	Number of Iterations/Time	Operating Time/Sec	CP/%	CR/%	QL/%
Method proposed in [6]	440	69.3	92.5	94.6	86.7
Method proposed in [7]	980	146.1	82.8	88.2	72.5
Method proposed in [8]	460	67.3	82.8	88.2	72.5
The proposed method	40	4.8	98.9	99.7	98.8

It can be seen from Figure 8, Figure 9, Figure 10 and Figure 11 that, the method proposed in this paper can extract the waterline accurately, especially the waterline of weak edges and serious concave edges, and it is featured with better stability, free from manual selection of seed points or initial boundary, with high level of automation. It can be seen from Figure 3, Figure 4, Figure 5 and Figure 6 that, the operating efficiency achieved by the method in this paper is significantly higher than that by the method specified in Literature [6-7] in terms of number of iteration and operation time, with the efficiency improved by more than 4 times; in terms of the extraction accuracy, the method proposed in this paper is higher in accuracy from 3 indicators like extraction completeness, accuracy and extraction quality.

Based on the analysis on the above 6 groups of experimental results, it can be obtained that: ① this paper utilizes the quad-tree segmentation to provide initial contour for curve evolution, realizing the automation of evolution; ② The signed pressure force function constructed in combination of the advantages of GAC, CV and LBF model has the capacity of dual-way evolution, thus improving the problem of GAC model effectively that it cannot extract the weak edges and serious concave edges at the same time, maintains the advantages of global information, avoids the minimum evolution contour locally, but also maintains the advantages of local information, so it has a better effectiveness in the segmentation of image with uneven gray scale; ③ Finally, the Selective Binary and Gaussian Filtering Level Set (SBGFRLS) method is

used to avoid reinitializing and regularization to improve the evolution efficiency; therefore, it is superior than other extraction methods in terms of efficiency and accuracy; ④The drawback lies in that the weight factor in the constructed signed pressure force function is decided by experience, which needs to be adjusted according to the details of the image and the nonuniformity of the gray scale.

4. CONCLUSIONS

In order to address the problem in waterline extraction from remote-sensing images that it is hard to extract the medium and weak edges and serious concave edges, or in long extraction time and low level of automation, this paper proposes a waterline extraction method based on quad-tree and multiple active contour models. The experimental results show that: this method can accurately extract the weak edges and serious concave edges, and owns the property of sub-pixel accuracy. Utilizes the highly efficient quad-tree segmentation method to obtain the initial contour of waterline, free from manual intervention, with high level of automation; improves the signed pressure force function and adopts Gaussian convolution and regularization level set function to avoid reinitialization, thus improving the waterline extraction efficiency significantly. As the algorithm in this paper is realized by matlab programming, the size of the image processed is limited, the larger images are considered to be divided into blocks or be processed by other methods; therefore, in-depth study will be made further in the future.

REFERENCES

- [1] Lee, S.hyun. & Kim Mi Na, (2008) "This is my paper", ABC Transactions on ECE, Vol. 10, No. 5, pp120-122.
- [2] Gizem, Aksahya & Ayese, Ozcan (2009) Coomunications & Networks, Network Books, ABC Publishers.
- [3] Joo-Hyung Ryu, Joong-Sun Won. Application of neural networks to waterline extraction in tidal flat from optic satellite images[C]. IEEE International Geoscience and Remote Sensing Symposium (IGARSS), 2002, 4: 2026–2028.
- [4] Ping Qin. Waterline information extraction from radial sand ridge of south yellow sea[C]. The 6th International Congress on Image and Signal Processing (CISP),2013:459–463.
- [5] Heng Li, Xinyu Wang. Automatic recognition of ship types from infrared images using support vector machines[C]. International Conference on Computer Science and Software Engineering, 2008, 6: 483–486.
- [6] WANG Min, LUO Jiancheng, MING Dongping. Extract ship targets from high spatial resolution remote sensed imagery with shape feature [J].Information science of wuhan university ,2005,30(8):685-688.
- [7] Zhen Li, Yongxue Liu, Manchun Li, etc. Automatic waterline pick-up based on improved embedded confidence[C]. The 18th International Conference on Geoinformatics,2010:1–6.
- [8] ZHANG Hongwei, ZHANG Baoming, GUO Haitao. An Automatic Coastline Extraction Method Based on Active Contour Model[J]. International Conference on Geoinformatics,2013,6:111-115.

- [9] SHEN Jiashuang, GUO Haitao, LI Haibin. A Water Edge Extraction Method from Images Based on Canny Operator and GAC Model[J]. *Journal of Geomatics Science and Technology*, 2013,30(3):264-268.
- [10] GUO Haitao, SUN Lei, SHEN Jiashuang, et al. An Island and Coastal Image Segmentation Method Based on Quadtree and GAC Model [J]. *Acta Geodaetica et Cartographica Sinica*.2016,45(1):65-72.
- [11] MinghongXie, Yafei Zhang and Kun Fu. Automatic Extraction of SAR Images Based on the Growth of Seed Points Coastline. *Journal of the Graduate School of the Chinese Academy of Sciences*, 2007, 24(1): 93-98.
- [12] SHEN Jiashuang. Research on Technology of Equal Waterline Information Extraction and Vertical Datum Transformation in Coastal Zone [D], PLA Information Engineering University,2008.
- [13] Wang X F. Level Set Method and Its Application in Image Segmentation [D]. University of Science and Technology of China, 2009 .().
- [14] Chan T F, Vase L A. Active contours without edges [J]. *IEEE Transactions on Images Precessing*.2001,10 (2) : 266-277.
- [15] Li C, Kao C Y, Gore J C, et al. Implicit active contours driven by local binary fitting energy[C]//Computer Vision and Pattern Recognition, 2007. CVPR'07. IEEE Conference on. IEEE, 2007: 1-7.
- [16] Li C, Kao C, Gore J C, et al. Minimization of region-scalable fitting energy for image segmentation. *IEEE Transactions on Image Processing*.2008,17(10):1940-1949.
- [17] Yun T, Mingquan Z, Fuqing D, et al. Efficient active contour model driven by statistical and gradient information[J]. *Journal of Image and Graphics*, 2011,16(8): 1489-1496.
- [18] Zhang K, Zhang L,Song H, et al. Active contours with selective local or global segmentation: a new formulation and level set method[J]. *Image and Vision computing*, 2010, 28(4): 668-676.
- [19] Wang X F, Min H. A level set based segmentation method for images with intensity inhomogeneity[M]//Emerging Intelligent Computing Technology and Applications. With Aspects of Artificial Intelligence. Springer Berlin Heidelberg, 2009: 670-679.
- [20] Su Rina, Wu Jitao. Refion-based Active Contour Model Improving The Signed Pressure Force Function[J].*Journal of Image and Graphics* ,2011,16 (12) : 2169-2174.
- [21] Fedkiw R, Osher S. Level set methods and dynamic implicit surfaces[J].Springer-Verlag, NewYork, 2002, 44: 77.
- [22] Y.Shi,W.C.Karl, Real-time tracking using level sets, *IEEE Conference on Computer Vision and Pattern Recognition*.(2005)34–41.
- [23] Zhang K, Song H, Zhang L. Active contours driven by local image fitting energy[J]. *Pattern Recognition*,2010,43 (4):1199- 1206.
- [24] DING Lei, YAO Hong,GUO Haitao, ,et al. Using Neighborhood Centroid Voting to Extract Road Centerline from High Resolution Image[J]. *Journal of Image and Graphics*,2015,20(11):1526-1534.

- [25] HE Zhonghai, WANG Baoguang, LIAO Yibai. Study of Method for Generating Ideal Edges[J]. Optics and Precision Engineering, 2002, 10(1): 89-93.
- [26] CHEN Xiaowei, XU Zhaohui, GUO Haitao, et al. Universal Sub-pixel Edge Detection Algorithm Based on Extremal Gradient[J]. Acta Geodaetica et Cartographica Sinica, 2014, 43(5): 500-507.

AUTHORS

Zhang Baoming (1961-). He is currently a full professor at Department of Photogrammetry and Remote Sensing, Zhengzhou Institute of Surveying and Mapping. His research interests are in the areas of digital photogrammetry, remote sensing, image processing, and pattern recognition.
Email: zbm1960@163.com



Guo Haitao (1976-), Ph.D. He is currently an associate professor at Department of Photogrammetry and Remote Sensing, Zhengzhou Institute of Surveying and Mapping. His main research interests include multi-temporal image processing and machine learning with applications to remote sensing image analysis.
Email: 15515768676@163.com



Lujun (1981-), Ph.D. He is currently a Lecturer at Department of Photogrammetry and Remote Sensing, Zhengzhou Institute of Surveying and Mapping. His research interests are related to digital photogrammetry and computer vision.
Email: ljhb45@126.com



Yu Jintao (1992-). He is currently a Master Degree Candidate at Department of Photogrammetry and Remote Sensing, Zhengzhou Institute of Surveying and Mapping. His research interests are related to object recognition from remote sensing images.
Email: 289386886@qq.com

